Article
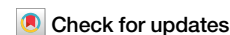
Regulating the metabolic flux of pyruvate dehydrogenase bypass to enhance lipid production in *Saccharomyces cerevisiae*

Check for updates

Cairong Lei[1,2], Xiaopeng Guo [3,5] ✉, Miaomiao Zhang [1,2,5] ✉, Xiang Zhou[1,2], Nan Ding[1,2], Junle Ren[1,2], Meihan Liu[1], Chenglin Jia[1,2], Yajuan Wang[1,2], Jingru Zhao[1,2], Ziyi Dong[1,2] & Dong Lu [1,2,4,5] ✉

To achieve high efficiency in microbial cell factories, it is crucial to redesign central carbon fluxes to ensure an adequate supply of precursors for producing high-value compounds. In this study, we employed a multi-omics approach to rearrange the central carbon flux of the pyruvate dehydrogenase (PDH) bypass, thereby enhancing the supply of intermediate precursors, specifically acetyl-CoA. This enhancement aimed to improve the biosynthesis of acetyl-CoA-derived compounds, such as terpenoids and fatty acid-derived molecules, in *Saccharomyces cerevisiae*. Through transcriptomic and lipidomic analyses, we identified *ALD4* as a key regulatory gene influencing lipid metabolism. Genetic validation demonstrated that overexpression of the mitochondrial acetaldehyde dehydrogenase (ALDH) gene *ALD4* resulted in a 20.1% increase in lipid production. This study provides theoretical support for optimising the performance of *S. cerevisiae* as a "cell factory" for the production of commercial compounds.

In recent years, microbial cell factories have been widely used to produce a myriad of chemicals and materials, including biofuels, bulk and fine chemicals, polymers, amino acids, natural products, and drugs[1]. To achieve high efficiency in microbial cell factories, central carbon fluxes are often redesigned to ensure a sufficient supply of precursors to produce high-value-added compounds[2]. Acetyl-CoA is an important intermediate metabolite in central carbon metabolism and a node where sugar metabolism flows to lipid molecule synthesis, which naturally becomes a precursor metabolite of many high-value compounds, such as fatty acid derivatives and terpenes[3]. In *Saccharomyces cerevisiae* (*S. cerevisiae*), acetyl-CoA is synthesised and consumed in a complex metabolic network distributed in four subcellular compartments (nucleus, cytoplasm, mitochondria, and peroxisomes), and acetyl-CoA cannot be transported directly among these compartments[4]. Increased mitochondrial and cytoplasmic acetyl-CoA levels are often prioritised (not the case during yeast fermentation)[1,5,6]. However, insufficient cytoplasmic acetyl-CoA biosynthesis often results in low production of these derivatives. In *S. cerevisiae*, Acetyl-CoA is synthesised via the PDH bypass pathway in the cytoplasm under fully fermentative conditions[7]. Therefore, to increase the supply of precursor acetyl-CoA, it is essential to rearrange the central carbon metabolic flux of the PDH bypass[2].

The PDH bypass comprises pyruvate decarboxylase (PDC), acetaldehyde dehydrogenase (ALDH), and acetyl-CoA synthetase (ACS)[8], which results in greater lipid production than does the PDH pathway[9]. Lipid synthesis is primarily dependent on an increase in cytoplasmic acetyl-CoA content by altering the ALDH reaction during PDH bypass, which is responsible for the oxidation of acetaldehyde to acetic acid and the conversion of $NAD(P)^+$ to $NAD(P)H$[10,11]. ALDH is divided into two groups: Mg^{2+}-activated, $NADP^+$ dependent, present in the cytoplasm; and K^+- and sulfhydryl-activated, NAD(P) dependent, present in the mitochondria (inhibited by glucose). Whole-genome sequencing of *S. cerevisiae* revealed five *ALDH* genes. *ALD6*, *ALD2*, and *ALD3* encode cytoplasmic ALDH[12,13], while *ALD4* and *ALD5* encode mitochondrial ALDH[14,15]. Ald6p and Ald4p are the major isomers dependent on Mg^{2+} and K^+, respectively. *ALD6* overexpression can enhance the entry of carbon fluxes into the PDH bypass pathway, drive carbon fluxes to acetyl-CoA, pull acetyl-CoA fluxes toward the target pathways, and downregulate the competing acetyl-CoA depletion pathway[1,3,16,17]. However, the function of *ALD4* in PDH bypass has rarely been reported.

[1]Institute of Modern Physics, Chinese Academy of Sciences, Lanzhou, China. [2]University of Chinese Academy of Sciences, Beijing, China. [3]School of Life Science and Engineering, Lanzhou University of Technology, Lanzhou, China. [4]Gansu Key Laboratory of Microbial Resources Exploitation and Application, Lanzhou, China. [5]These authors jointly supervised this work: Xiaopeng Guo, Miaomiao Zhang, Dong Lu. ✉e-mail: guoxpmicrobio@126.com; zhangmiaomiao@impcas.ac.cn; ld@impcas.ac.cn

ALD4 is essential for anaerobic glucose fermentation to acetic acid in *S. cerevisiae* and is associated with cell growth on ethanol[18,19]. Overexpression of *ALD4* can increase the production of 3-hydroxypropionic acid (3-HP) and 1,3-propylene glycol via biological fermentation. Notably, the heterologous expression of *ALD4* enables the production of 3-HP using glycerol as a substrate, which can be used to synthesise many important chemical products[20,21]. Moreover, *ALD4* is a key target gene for enhancing furfural tolerance, thereby improving the utilisation of lignocellulose by *S. cerevisiae*[22]. During anaerobic fermentation, *ALD4* expression is elevated in response to under high ethanol exposure and glucose depletion[12,23]. In glycerol biosynthesis, knocking out *ALD6* in the cytoplasm results in the reduction of most NADH, although some NADH is still supplied by mitochondrial *ALD4*[12,24]. The *ALDH* gene superfamily is responsible for catalysing the irreversible oxidation of endogenous and exogenously produced aromatic and aliphatic aldehydes. These genes play a crucial role in various fundamental biomolecular synthesis pathways, including the synthesis of vitamins, carbohydrates, amino acids, and lipids[25]. However, the relationship between *ALD4* and lipid metabolism has not been well-characterised.

Therefore, we hypothesised that *ALD4*, similar to *ALD6*, can alter the direction of carbon flux in the PDH bypass, promote the assimilation of ethanol, and affect the synthesis of acetyl-CoA and downstream lipid metabolites. Our study highlights a novel aspect of *ALD4* function by demonstrating its role in enhancing the Crabtree effect through the regulation of acetaldehyde flow to ethanol synthesis. Unlike previous studies that primarily focus on the involvement of *ALD4* in acetic acid production, glycerol metabolism, and furfural tolerance[18–22], our findings provide new insights into how *ALD4* overexpression can significantly alter metabolic pathways under aerobic conditions, thereby promoting fermentation even in the presence of oxygen. This study aimed to identify a metabolic engineering strategy that increases lipid synthesis by *S. cerevisiae* during anaerobic fermentation. Multi-omics analyses are conducted to identify important regulatory genes that are responsible for increasing lipid synthesis. The synthesis of acetyl-CoA and lipids was effectively promoted by regulating the flow of glycolytic carbon flux to PDH bypass pathway. Our study provides new insights and directions for further development of PDH bypass-based metabolic engineering strategies to enhance the microbial synthesis of industrial lipid compounds.

Results

Association analysis between lipidome and transcriptome reveals DEGs potentially affecting lipid metabolism

Through a combination of genomic, transcriptomic, and lipidomic analyses, we have previously revealed that the changes in lipid metabolism observed in populations of mitochondrial respiration-deficient mutants (MRDMs) are attributable to mitochondrial dysfunction (Fig. 1)[26]. In this study, to identify the genes involved in lipid metabolism, we analysed the differentially expressed genes (DEGs) and differentially expressed metabolites (DEMs) in MRDMs that were exposed to heavy-ion radiation. Three MRDM (ResD-1, ResD-2, and ResD-4) strains were selected; 25 lipid subclasses and 648 lipid molecules were quantified via nontargeted lipidomic analysis (Fig. S1). Principal component analysis (PCA) revealed a high degree of inter-group variability between the control and mutant groups (Fig. 2A). Univariate analysis can intuitively show the significance of lipid changes between two groups. Volcano map analysis that mitochondrial damage caused significant changes in lipid metabolites (Fig. 2B). By comparing the relative contents of different lipid subclasses, we found that the relative contents of fatty acyls (FA), glycerophospholipids (GP) and glycerolipids (GL) in ResD-1, ResD-2, and ResD-4 were significantly greater than those in the control group (Fig. 2F–J). Among them, the proportion of significant changes in the single neutral lipid TG was the greatest, and TG was the heavy energy storage and energy supply fat in yeast cells[27]. In addition to TG, PE, PC, PS, and PI were significantly different. These four polar lipids are important components of the cell membrane of *S. cerevisiae* (Fig. S2).

To further identify key genes involved in lipid metabolism, the top 20 pathways with the lowest significant *q* values were selected on the basis of the KEGG pathway annotations. We identified several lipid metabolic pathways that are most affected in MRDMs, including fatty acid, GL and GP metabolism (Fig. 2C–E). There were 35 lipid metabolism-related DEGs involved in these pathways, most of which were significantly downregulated, indicating that mitochondrial damage caused lipid metabolism disorders. In contrast, *ALD4* was significantly upregulated and annotated to two metabolic pathways, fatty acid biosynthesis and degradation and GL metabolism (Fig. 2K). These results suggest that the upregulation of *ALD4* is associated with increased FA and GL contents and that *ALD4* can serve as a key regulatory gene for lipid metabolism in yeast (Fig. 1).
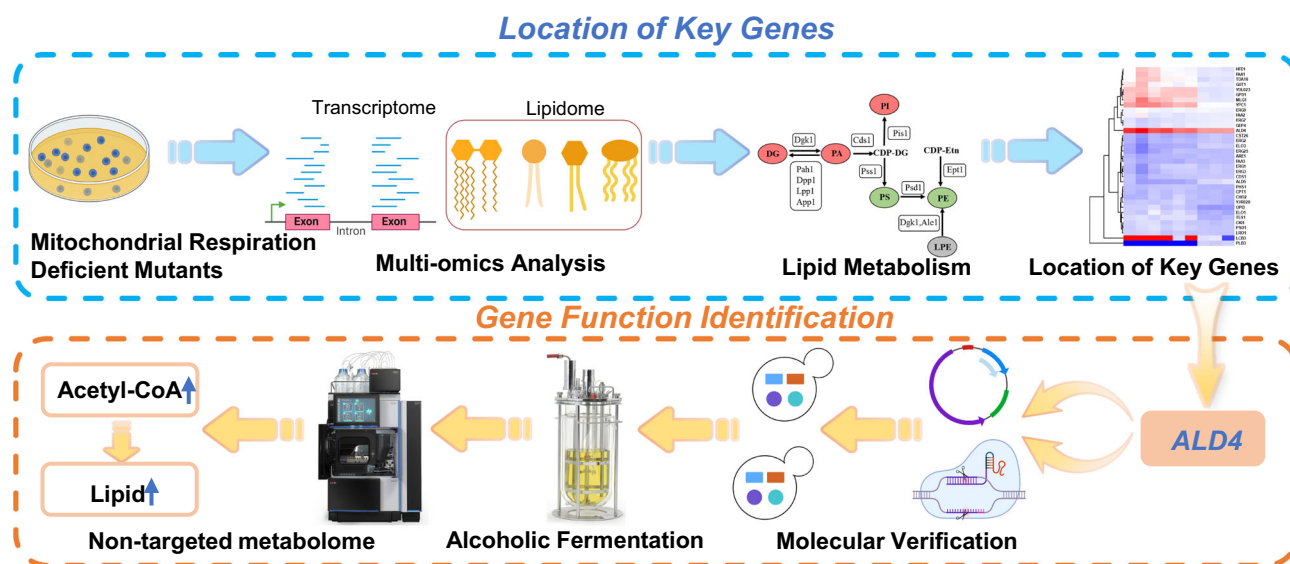
Fig. 1 | Construction of key functional gene analysis platform. Based on population data, biological information involving multiple genes and traits can be obtained with high throughput. The phenome, genome, transcriptome, and metabolome combination strategy were used to further target key functional genes, and the metabolic pathways in which the genes reside and specific biological function changes were understood in detail. Finally, the function of key genes was verified using gene knockout or overexpression, which confirmed that the candidate genes that were mined truly regulated the target phenotype. (Some icons created in BioRender).
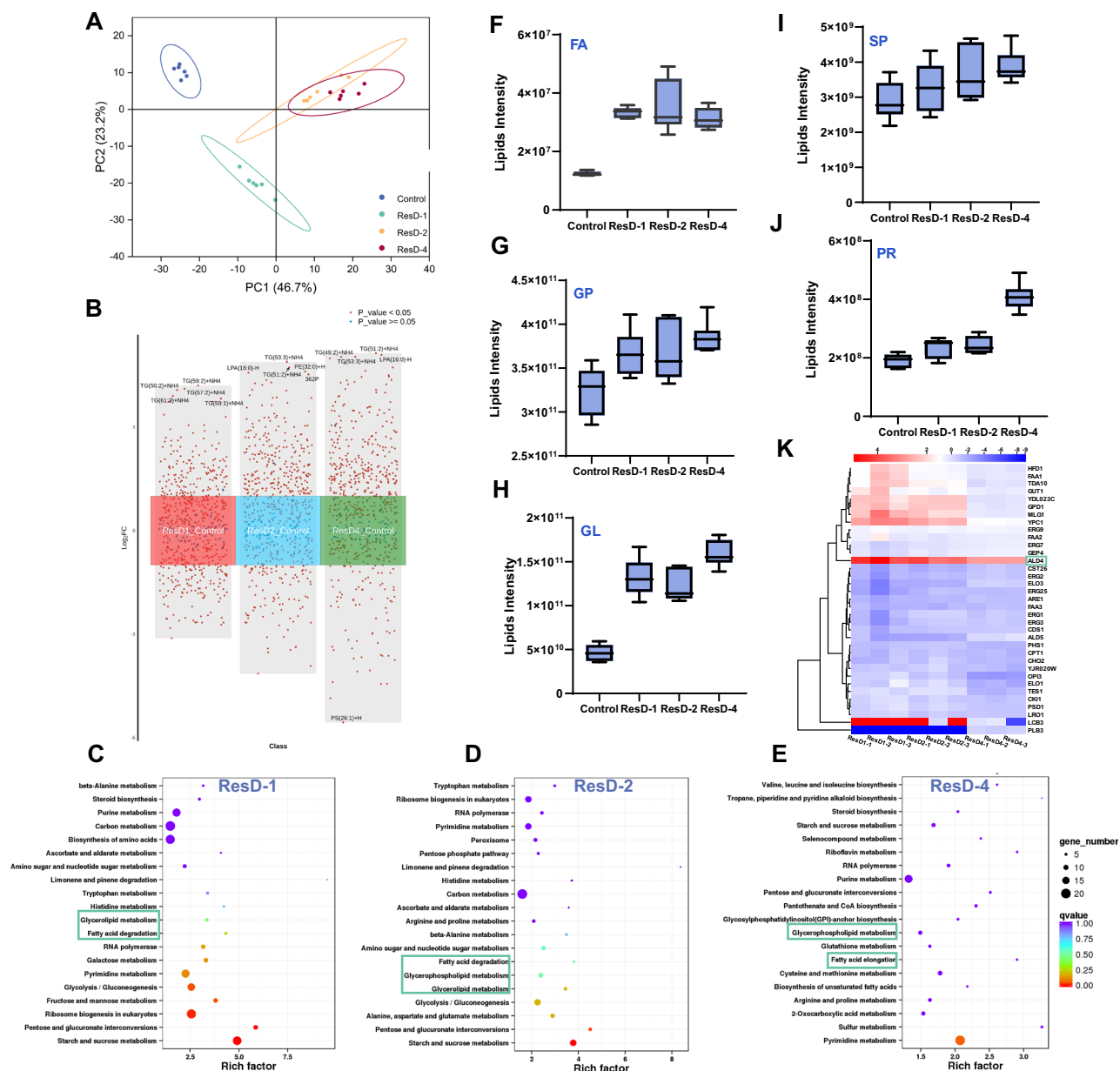
Fig. 2 | Lipidome and transcriptome analysis of MRDMs (Resd-1, Resd-2, and Resd-4). A PCA score plot of the MRDM/control group, PCA primary component analysis, MRDM mitochondrial respiration-deficient mutants. **B** Univariate analysis, volcano plot of the MRDM/control group data, and DEM screening (FC > 2.0, $p < 0.05$); DEMs differentially expressed metabolites. Based on the KEGG pathway annotations, the top 20 pathways with the lowest significant Q values were obtained (**C**: ResD-1, **D**: ResD-2, **E**: ResD-4). **F** Relative contents of fatty acyls (**F–J** all included six biological replicates). **G** Relative glycerophospholipid content. **H** Relative glycerolipid content. **I** Relative contents of sphingolipids. **J** Relative contents of prenol lipids. **K** Heatmap of DEGs related to lipid metabolism; DEGs differentially expressed genes. Error bars represent standard error (SE).

ALD4 negatively regulates both ethanol synthesis and the alcohol fermentation

To accurately determine the phenotypic effects of *ALD4*, we generated *ALD4*-overexpressing (*ald4-oe*) and *ALD4*-knockout (*Δald4*) strains (Fig. S3). Growth curve experiments in yeast extract peptone dextrose (YPD) medium with 2% glucose showed no significant growth differences among the strains (Fig. 3A). In ethanol fermentation medium with 20% glucose, we measured ethanol production, residual sugar content, and CO_2 production at 72 and 96 h. At 72 h, the *ald4-oe* strain showed an 8.10% decrease in ethanol concentration compared to the control, while *Δald4* showed a 6.33% increase (Fig. 3C). Correspondingly, the *ald4-oe* strain exhibited a 9.55% increase in residual sugar and reduced CO_2 production, indicating inhibited fermentation, whereas *Δald4* displayed a 15.29% reduction in residual sugar and increased CO_2

production, indicating enhanced fermentation (Fig. 3B, D). These trends continued at 96 h, further supporting that *ALD4* overexpression inhibits ethanol synthesis and the fermentation process (Fig. 3G). Moreover, the *Δald4* mutant grew slightly slower than the parental strain in media supplemented with ethanol as the sole carbon source, and its tolerance to ethanol was significantly reduced (Fig. 3E, F), which was consistent with the findings of Wang et al.[15]. Discrepancies regarding the ability of *Δald4* mutants to grow on ethanol exist[14,15]. The *Δald4* mutants created by Tessier et al.[14] could not grow on ethanol, whereas our *Δald4* mutants could. This is because when the cytoplasmic ALDH activity is sufficient, yeast can compensate for the deficiency of mitochondrial ALDH in ethanol media. When mitochondrial enzymes are present as a source of energy, cytoplasmic ALDH cannot compensate[28].
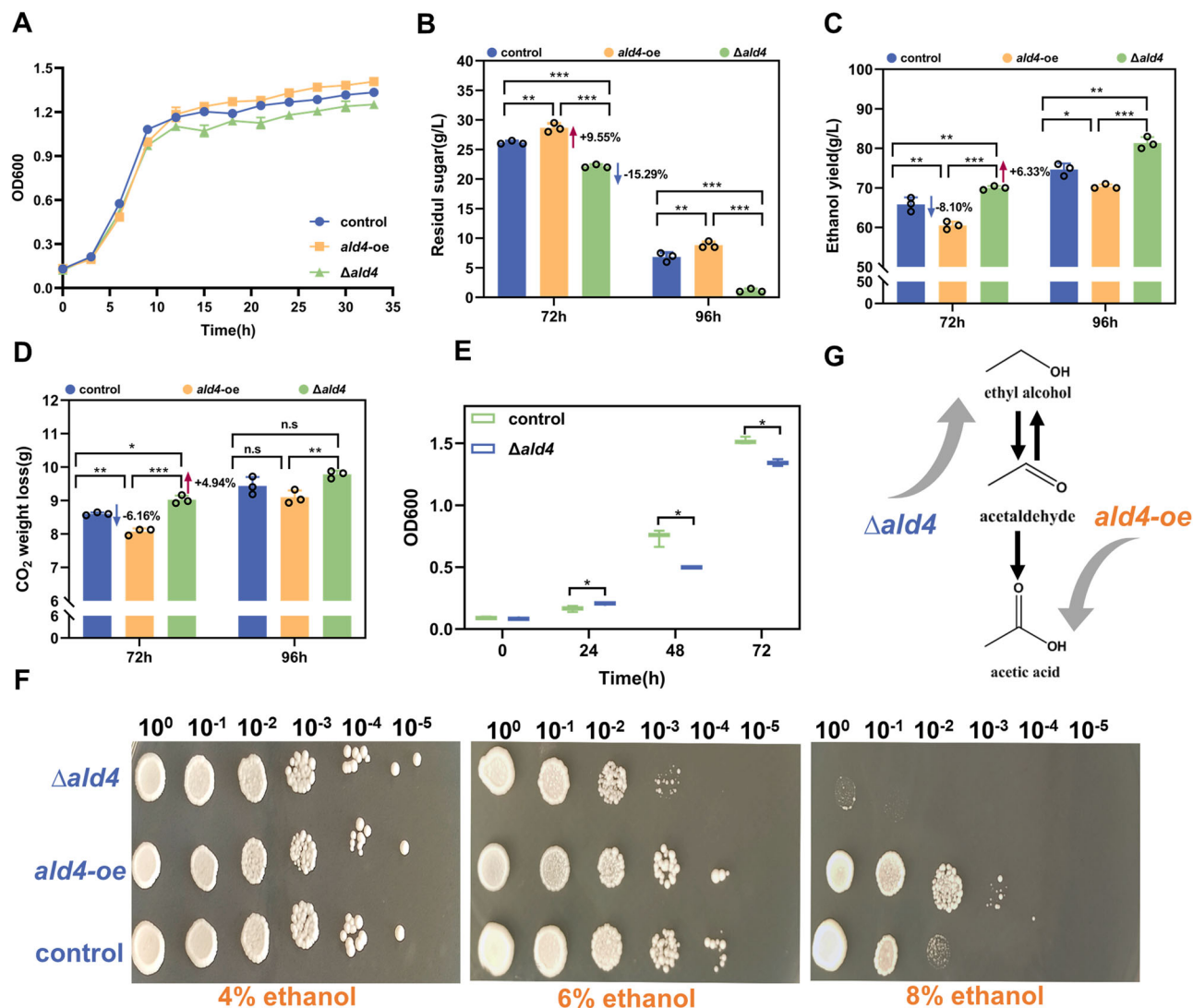
Fig. 3 | Growth and fermentation of the *ald4-oe* and *Δald4* strains. A Growth curves (n = 3 biological replicates) in YPD medium with 2% glucose. Measurements were taken every 3 h for 36 h. **B** Residual sugar content (n = 3 biological replicates, **p = 0.001, **p = 0.005, ***p < 0.001) in ethanol fermentation medium containing 20% glucose. Measurements were taken at 72 and 96 h. **C** Ethanol yield (n = 3 biological replicates, *p = 0.017, **p = 0.001, **p = 0.005, ***p < 0.001). **D** CO_2 weight loss (n = 3 biological replicates, $^{n.s}p$ = 0.088, $^{n.s}p$ = 0.083, *p = 0.011, **p = 0.004, **p = 0.006, ***p < 0.001). **E** Growth of the *Δald4* strain in ethanol liquid medium (n = 3 biological replicates, *p = 0.044, *p = 0.025, *p = 0.024). **F** Ethanol stress tolerance of strains (the ethanol volume fractions were 4%, 6%, and 8%). **G** Schematic diagram of *ALD4* overexpression or knockout affecting acetaldehyde flow. Error bars represent standard error (SE).

ALDH positively impacts acetyl-CoA biosynthesis as a key enzyme of PDH bypass

Based on regulating the expression of *ALD4* encoding mitochondrial ALDH, we measured the activity of different enzymes in the PDH bypass pathway and the expression levels of their coding genes (Table 1). K⁺-ALDH and alcohol dehydrogenase (ADH) enzyme activity increased significantly in the *ald4-oe* strain (Fig. 4A, C). *ADH1* expression decreased significantly, whereas *ALD4* and *ADH2* expression increased significantly (Fig. 4F, G). *ADH1* and *ADH2* are responsible for ethanol production and ethanol conversion to acetaldehyde, respectively. In contrast, the K⁺-ALDH and ADH enzyme activities of the *Δald4* strain were significantly inhibited, and *ADH1* expression increased significantly. *ALD4* and *ADH2* decreased significantly. These results indicated that *ALD4* overexpression promotes acetaldehyde and acetic acid synthesis, whereas *ALD4* knockout promotes ethanol synthesis. The activity of the Mg²⁺-ALDH enzyme and corresponding genes did not change, while only PDC enzyme activity of the *Δald4* strain decreased significantly (Fig. 4B, D, F, H), suggesting that *ALD4* knockout may

reduce the carbon flux from glycolysis to PDH bypass. Overall, these findings suggest that *ALD4* is mainly responsible for regulating acetaldehyde flow into the mitochondria through the use of K⁺-ALDH to form acetate, and the generated acetate is transported out of the mitochondria into the cytoplasm to form acetyl-CoA. *ALD4* knockout regulated acetaldehyde flow to ethanol synthesis, thus enhancing the Crabtree effect. These findings are consistent with those of Miyagi et al.[29].

Particularly, in the *ald4-oe* strain, the level of acetyl-CoA was significantly increased by ~17% compared with that in the parental strain, and *ACS2* gene expression was significantly upregulated (Fig. 4E, I). Elevated levels of *ACH1* and *ACC1* transcripts were observed in *ald4-oe* cells (Fig. 4J). Chen et al.[30] showed that *ACH1* overexpression increased acetyl-CoA levels in the cytoplasm by increasing acetic acid levels in the mitochondria. *ACC1* encodes acetyl-CoA carboxylase, which catalyses cytoplasmic acetyl-CoA carboxylation to malonyl-CoA and plays an important role in fatty acid and polyketide (PK) compound synthesis[4]. These results suggest that the alteration of *ALD4* leads to global shifts in carbon flux with the potential to increase value-added metabolites.

Table 1 | List of DEGs in PDH bypass

Gene name	Coding protein name	Function description	Primer sequences
ALD4	Mitochondrial aldehyde dehydrogenase	Required for growth on ethanol and conversion of acetaldehyde to acetate	F: CCTTCCTATGACAGTGCCTATC R: CTCTTCCACATCGTCCTCTC
ALD6	Cytosolic aldehyde dehydrogenase	Required for conversion of acetaldehyde to acetate	F: TAAGAGATGCTGCTGCCTATG R: TGACCACAGACACCGATTG
ADH1	Alcohol dehydrogenase	Required for the reduction of acetaldehyde to ethanol	F: TGATGGCCGGTCACTGGGTT R: ACCTTCACCACCGTCAATACCCA
ADH2	Glucose-repressible alcohol dehydrogenase II	Catalyses the conversion of ethanol to acetaldehyde	F: GCTGAAGTCGCGCCAATCTTGT R: AGCAGCACCAGAAATGGCCG
PDC1	Major of three pyruvate decarboxylase isozymes	Key enzyme in alcoholic fermentation; decarboxylates pyruvate to acetaldehyde	F: CTATTGCTGACGCCGCTAA R: CTATTGCTGACGCCGCTAA
PDC5	Minor isoform of pyruvate decarboxylase	Key enzyme in alcoholic fermentation, decarboxylates pyruvate to acetaldehyde	F: GCTGCCTATGCTGCTGAT R: TTGAGAAGAGATGGATGGAACAC
PDC6	Minor isoform of pyruvate decarboxylase	Decarboxylates pyruvate to acetaldehyde	F: AACGCTACGTTCCTCGGTGT R: TTGGTTGGTACGGGAACGCT
ACS1	Acetyl-coa synthetase isoform	Expressed during growth on nonfermentable carbon sources and under aerobic conditions	F: GCGATACTGTTGCCGTGTA R: ACCTCTGTTGGATTCATCTGTAG
ACS2	Acetyl-coa synthetase isoform	Required for growth on glucose, expressed under anaerobic conditions	F: TGATGACGAATCCGACAACAA R: AGCCACAGCCAACATAGC
ACC1	Acetyl-CoA carboxylase	Catalyses carboxylation of cytosolic acetyl-CoA to form malonyl-CoA	F: AAGGTGTTGTCGTTGGTAGAG R: CAGTCTTGAAGGCGGAGTT
ACH1	Mitochondrial acetyl-coenzyme A carboxylase	Catalyses production of malonyl-CoA in mitochondrial fatty acid biosynthesis	F: AACAACAACAATTACGCCAACA R: CCAGGAGGACCAATGAATAGTATT

The italic format indicates the gene name.

Metabolic profiling of *ALD4*-overexpressing or knockout lines

To qualitatively and quantitatively investigate the multicomponent dynamic response of metabolite levels in vivo owing to *ald4* mutation, 1452 metabolites were quantified using an ultrahigh-performance liquid chromatography (UPLC) tandem high-resolution mass spectrometer. The orthogonal partial least squares-discriminant analysis showed that the model was stable and reliable (Fig. S4), and the DEMs were screened according to the projected importance of the variables (VIP). In the *ald4-oe* and Δ*ald4* groups, 642 and 755 DEMs were identified, respectively (Fig. 5A). PCA of all DEMs revealed inter-group and intra-group variability at the population level. Parallel samples from each group were collected (Fig. 5B), indicating that the instrument has stable performance, good experimental repeatability, and reliable detection data. The different samples exhibited a good distribution among the groups. KEGG-annotated metabolite enrichment analysis was used to investigate whether *ald4* mutations affect specific metabolite groups. As expected, lipid metabolism was the main metabolite class affected, especially linoleic acid and arachidonic acid (polyunsaturated fatty acid) metabolism (Fig. 5F). Subsequently, the differentially expressed lipid metabolites (DELMs) involved in the two groups of DEMs were classified and statistically analysed. Figure 5C–E illustrates the detection of lipid subclasses, the proportions of lipid subclasses, and the number of lipid metabolites present in each subclass. In total, 109 and 119 lipid molecules were annotated in the *ald4-oe* (Supplementary Table 1) and Δ*ald4* groups (Supplementary Table 2), respectively, and were classified into five categories: FA, GP, prenol lipids (PR), PK, and sterol lipids (ST) (Fig. 5C). Compared with the parent strain, the *ald4-oe* strain had 13.6% greater FA content, and the Δ*ald4* strain had 8.09% lower FA content. In contrast, the PK content of the Δ*ald4* strain increased by 29.8%, while that of the *ald4-oe* strain did not change significantly (Fig. 5D, E). The changes in the contents of the other lipid subclasses were the same except for those of the above two lipid subclasses. In general, cytoplasmic acetyl-CoA in *S. cerevisiae* is mainly catalysed by acetyl-CoA carboxylase (*ACC1*) to synthesise malonyl-CoA, which is mainly used for the biosynthesis of fatty acids or PK. Therefore, *ALD4* overexpression increased acetyl-CoA production and the NADPH supply, providing more carbon donors and energy for fatty acid synthesis, while *ALD4* knockout reduced the metabolic flow of fatty acid synthesis but promoted PK synthesis. The synthesis of PK by microorganisms is usually limited because fatty acids are considered byproducts that withdraw malonyl-CoA[31].

Spearman correlation coefficients were calculated to measure the correlations between metabolites and observe the consistency of DELMs (FC > 2) trends. The content of FA, specifically arachidonic acid, hydroxy fatty acids, and FA carnitines, increased significantly in the *ald4-oe* group (Fig. 5G). Owing to their potential medicinal and nutritional effects, both linoleic and arachidonic acids (18–22 carbon unsaturated fatty acids) have recently attracted great interest[32]. However, the correlation between the metabolites of FA was low, and we did not observe synergistic or mutually exclusive relationships (Fig. 5H). In contrast, PK and GP levels increased significantly in the Δ*ald4* group, with the greatest increase observed in macrolide and lactone PK levels (Fig. 5G). Most metabolites exhibited similar positive correlation trends in both groups (Fig. 5I). These results further highlight the association of *ALD4* with lipid metabolites and confirm that *ALD4* mutations differentially regulate lipid metabolite distribution systems.

Discussion

Recently, increasing the titre, yield, and productivity of lipid derivatives in *S. cerevisiae* and other eukaryotic microorganisms has attracted extensive attention[33]. Increasing cytoplasmic acetyl-CoA levels by regulating mitochondrial PDH complexes or introducing PDH bypass pathways has been prioritised[34]. In this study, we promoted the synthesis of acetyl-CoA by regulating the distribution of carbon flux during yeast PDH bypass, which significantly increased the content of FA metabolites. Overexpressing *ALD4* increased acetyl-CoA and fatty acid levels by 17.10% and 13.6%, respectively. This is the first time for yeast (to the best of our knowledge) that *ALD4* has been shown to affect cytoplasmic acetyl-CoA synthesis, which is involved in the synthesis of important lipid compounds.

We used several methods of analyses to identify key genes that are involved in lipid metabolism. First, multi-omics analysis was used to target candidate genes. The transcriptome and lipidome analysis revealed differences in lipid metabolite regulatory networks following mitochondrial damage in yeast cells. Significant upregulation of the target gene, *ALD4*, was accompanied by a marked increase in FA and GL lipid content (Fig. 2). With regards to the lipid metabolism synthesis target pathway, most precursor
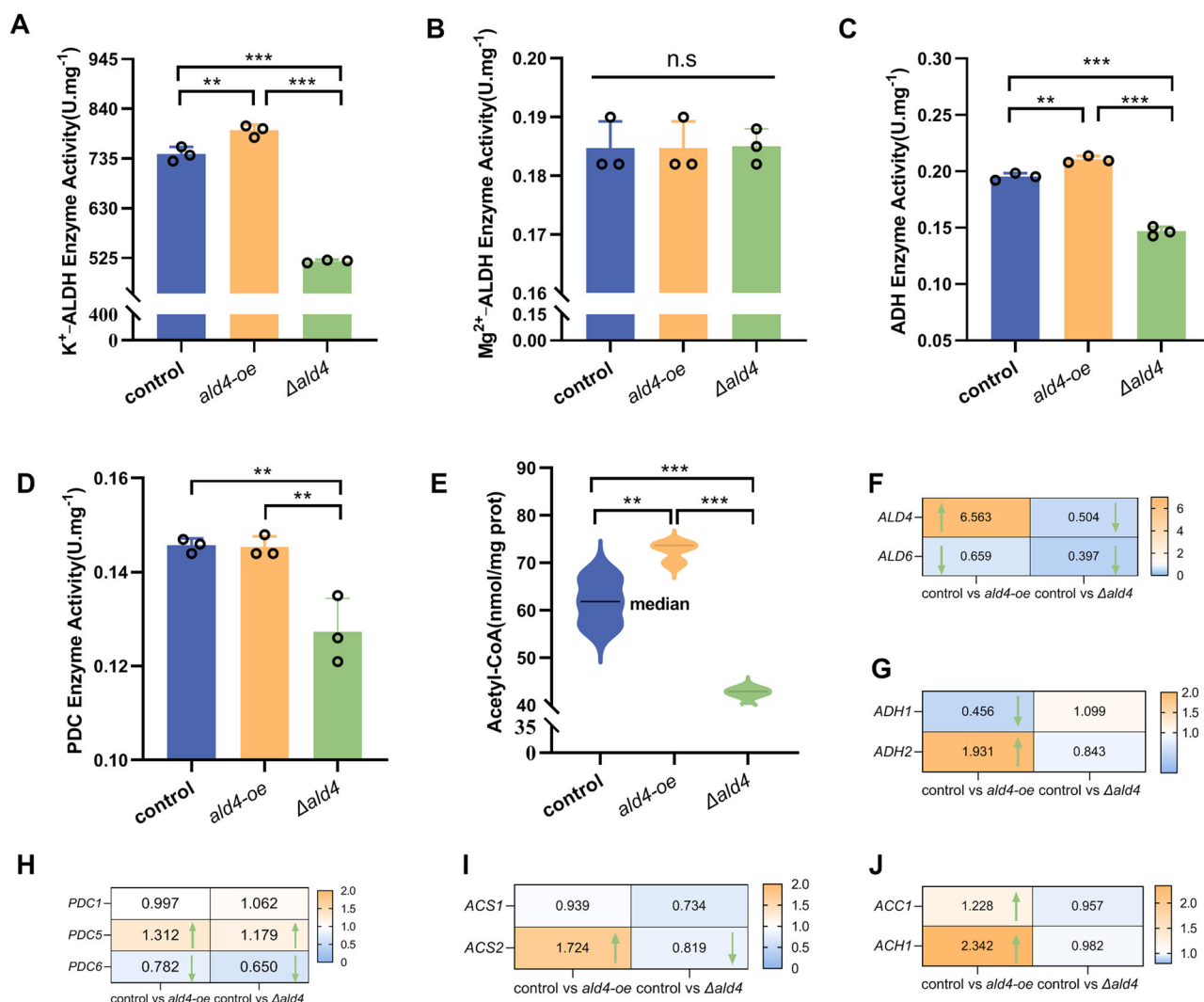
Fig. 4 | Measurement of key enzyme activities and PDH bypass gene expression after 72 h of fermentation in ethanol medium. A Mitochondrial ALDH enzyme activity ($n = 3$ biological replicates, ***$p < 0.001$, **$p = 0.002$), ALDH acetaldehyde dehydrogenase. **B** Cytoplasmic ALDH enzyme activity ($n = 3$ biological replicates, n.s$p = 0.180$, n.s$p = 0.917$, n.s$p = 0.209$). **C** ADH enzyme activity ($n = 3$ biological replicates, ***$p < 0.001$, **$p = 0.002$), ADH alcohol dehydrogenase. **D** PDC enzyme activity ($n = 3$ biological replicates, **$p = 0.002$), PDC pyruvate decarboxylase. **E** Acetyl-CoA content ($n = 3$ biological replicates, ***$p < 0.001$, **$p = 0.009$). **F** qPCR of ALDH-encoding genes. **G** qPCR of ADH-encoding genes. **H** qPCR of PDC-encoding genes. **I** qPCR of ACS-encoding genes; ACS acetyl-CoA synthetase. **J** qPCR of other genes. Error bars represent standard error (SE).

molecules of lipid compounds are derived from cytoplasmic acetyl-CoA, which is dependent on PDH bypass. Nevertheless, the pyruvate produced during glycolysis is mainly converted to ethanol by cytoplasmic PDC rather than acetyl-CoA via the PDH bypass (Crabtree effect)[35]. Therefore, we focused on regulating the carbon flow distribution toward the PDH bypass, with the aim of reducing ethanol production, transferring the carbon flux to acetaldehyde and increasing the acetaldehyde supply.

Various approaches have been explored to enhance cytoplasmic acetyl-CoA supply, including overexpression strategies to promote the conversion of ethanol to acetaldehyde[4,36], knockout methods to limit the reduction of acetaldehyde to ethanol[37], and the overexpression to promote the conversion of acetaldehyde to acetic acid[4,38]. However, the potential of regulating mitochondrial ALDH, as a PDH bypass branch, to increase the cytoplasmic acetyl-CoA supply has not been thoroughly investigated. Compared to methods such as *ADH2* overexpression, *ADH1* knockout, or *ALD6* overexpression, targeting mitochondrial ALDH offers advantages in specificity and efficiency[39]. Mitochondrial ALDH directly impacts the REDOX balance within the mitochondria, increasing NADPH levels and enhancing the production of acetyl-CoA. This approach avoids the potential metabolic imbalances that might arise from altering the expression of cytosolic

enzymes such as *ADH2* or *ALD6*. Moreover, overexpressing or knocking out *ADH2* can have broader systemic effects, as these enzymes are heavily involved in ethanol metabolism and other cellular processes[18]. Overexpressing *ALD6*, a cytosolic enzyme, might not be as effective in increasing acetyl-CoA levels within the mitochondria, where it is most needed for energy production and metabolic functions[8]. The main rate-limiting step for acetyl-CoA production in our system appears to be the availability of NADPH, which is essential for the activity of several dehydrogenase enzymes involved in acetyl-CoA synthesis pathways. By increasing NADPH through the regulation of mitochondrial ALDH (overexpression of *ALD4*), acetyl-CoA production can be effectively enhanced.

In addition to the significant upregulation of *ALD4*, other genes such as *LCB3*, *YPC1*, *MLO1*, and *YDL023C* also exhibited notable upregulation trends (Fig. 2K). *LCB3* encodes a long-chain base kinase involved in the sphingolipid biosynthetic pathway. Its upregulation indicates increased sphingolipid metabolism, which may play a role in cell signalling and membrane structure stability, thereby affecting cellular stress responses and overall cell homoeostasis[40]. *YPC1* encodes an alkaline ceramidase that hydrolyses ceramide into sphingosine, and its upregulation suggests enhanced ceramide metabolism, which can influence apoptosis, cell cycle
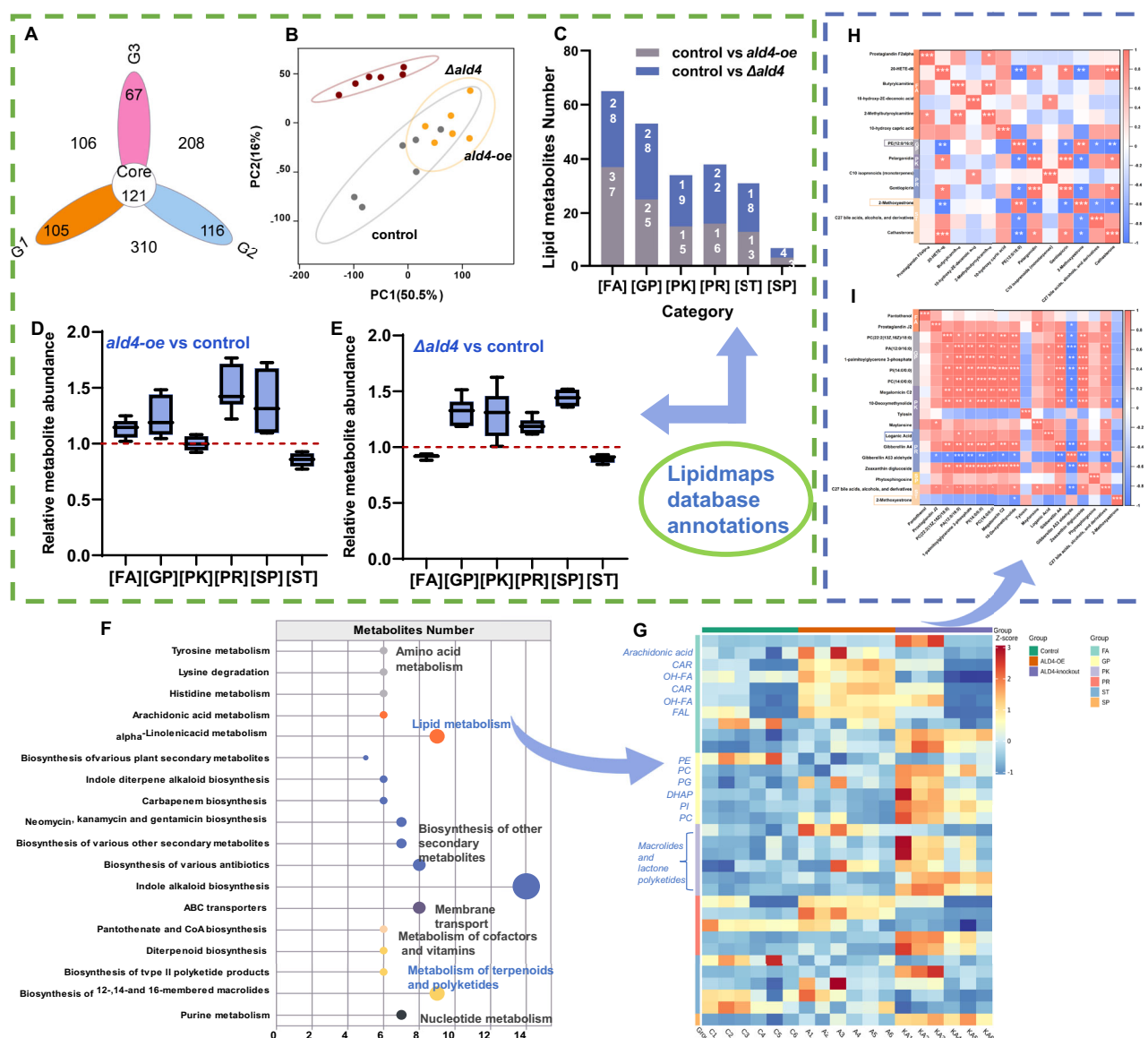
Fig. 5 | Metabolomic analysis of *ald4-oe* and *Δald4* strains after 72 h of fermentation in ethanol medium. A DEM statistical Venn diagram, DEM screening (FC > 1.0, VIP > 1.0, *p* < 0.05), DEMs differentially expressed metabolites. G1: *ald4-oe* vs control, G2: *Δald4* vs control, and G3: *ald4-oe* vs *Δald4*. **B** PCA score plot of the *ald4-oe/Δald4*/control group. **C** DELM classification statistics, DELMs differentially expressed lipid metabolites, FA fatty acyls, GP glycerophospholipids, PK polyketides, PR prenol lipids, SP sphingolipids, ST sterol lipids. **D** The relative content of different lipid subclasses in the *ald4-oe* group vs the control group. **E** The relative content of different lipid subclasses in the *Δald4* vs control groups. **F** Annotation of all identified metabolites using the KEGG database. The top 20 annotations with the most annotations of the KO pathway-level entries were selected, and a summary bar chart was constructed. **G** Heatmap of DELMs (FC > 2.0, VIP > 1.0, *p* < 0.05, *n* = 6 biological replicates). **H** Correlation analysis between DELMs in the *ald4-oe* group. **I** Correlation analysis between DELMs in the *Δald4* group. Error bars represent standard error (SE).

regulation, and stress responses, thus indicating a possible protective mechanism against cellular stress[41]. *MLO1* encodes a member of the mitochondrial carrier family responsible for transporting metabolites across the inner mitochondrial membrane. Its upregulation implies enhanced transport activity, potentially improving mitochondrial function and efficiency in metabolite exchange, thus supporting increased acetyl-CoA synthesis[42]. Although the function of *YDL023C* is not well-characterised, it is believed to be involved in various cellular processes, including protein folding and stress responses. Its upregulation may indicate an adaptive response to maintain protein homoeostasis and cellular integrity under conditions that promote increased acetyl-CoA production[43]. In summary, the upregulation of these genes, along with *ALD4*, suggests a coordinated cellular response to optimise metabolic pathways and maintain homoeostasis. The increased expression of *LCB3* and *YPC1* suggest enhanced sphingolipid metabolism, which could play roles in signalling and stress

response. Moreover, the upregulation of *MLO1* indicates improved mitochondrial transport activity, supporting acetyl-CoA synthesis. Finally, the upregulation of *YDL023C* may reflect a broader adaptive response to ensure cellular integrity under changing metabolic conditions.

The biological function of *ALD4* in yeast was evaluated using knockout and overexpression experiments. We found that *ALD4* overexpression increased mitochondrial ALDH enzyme activity, inhibited ADH enzyme activity, restricted acetaldehyde conversion to ethanol, and promoted the conversion of acetaldehyde to acetic acid. Furthermore, the generated acetic acid was transferred to the cytoplasm and became a precursor molecule for acetyl-CoA synthesis (Fig. 6A). Cytoplasmic acetyl-CoA is mainly used in the synthesis of fatty acids or their derivatives[44]. The products derived from acetyl-CoA have various applications in the energy and chemical industries, agriculture, pharmaceuticals, and other fields[45,46]. Moreover, acetyl-CoA is involved in the synthesis of GP, sterol esters, PR, and PK compounds, which
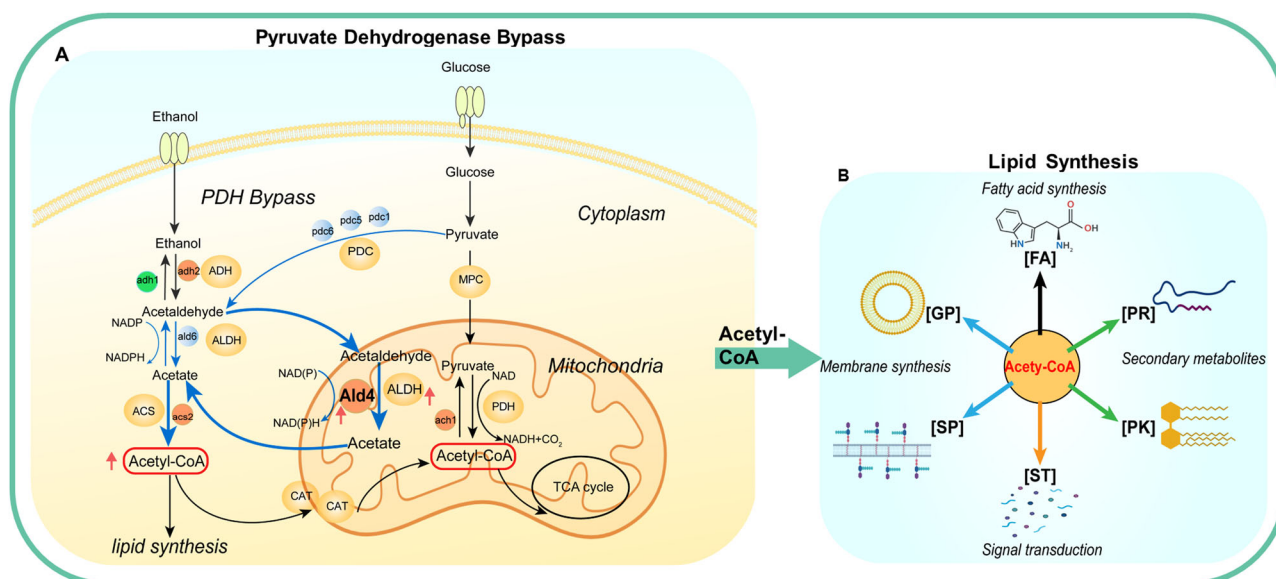
Fig. 6 | Schematic representation of acetyl-CoA synthesis through the PDH bypass and its impact on lipid metabolites. A The influence of *ALD4* over-expression on the PDH bypasses key enzyme activity and key genes. *ALD4* over-expression increased mitochondrial ALDH enzyme activity, inhibited ADH enzyme activity, and promoted acetaldehyde conversion to acetic acid, and the generated acetic acid was transferred to the cytoplasm and became a precursor molecule for acetyl-CoA synthesis. The orange circles, green circles, blue circles, yellow ovals, blue arrows, and bold arrows indicate gene upregulation, gene downregulation, non-significant gene changes, enzymes encoded by genes, PDH bypass, and increased metabolic flux, respectively. **B** In the metabolome of *ald4-oe* strains, significant changes in the levels of different lipid compounds were detected. The black, green, orange, and blue arrows indicate fatty acid synthesis, synthesis of major secondary metabolites, synthesis of hormone molecules responsible for signalling, and biofilm synthesis, respectively. (Some icons created in BioRender).

help maintain the integrity of the cell membrane[47]. It also participates in cell signalling and the formation of important secondary metabolites such as terpenoids, quinones, and phenols (Fig. 6B). Based on these findings, our study indicates that ALDH expression enhances intracellular acetyl-CoA synthesis and further modulates lipid metabolic pathways. Given the high correlation between acetyl-CoA synthesis and NADPH/NADP^{+} and ATP/ADP ratios, the regulatory effect of ALDH may be related to changes in cellular energy homoeostasis and REDOX balance[9]. Thus, direct measurements of NADPH/NADP^{+} and ATP/ADP ratios in future studies will be essential for achieving a more comprehensive understanding of the regulatory role of ALDH in cellular metabolism and REDOX equilibrium.

In general, increasing *S. cerevisiae* cytoplasmic acetyl-CoA levels should not solely be considered a strategy to reduce the Crabtree effect because of the constraints imposed by ACS inhibition, low enzyme activity, and the demand for ATP, all of which collectively limit acetate production[48]. To improve *S. cerevisiae* cytoplasmic acetyl-CoA levels from different aspects and the synthesis of related derivatives, several methods have been proposed. (1) Key gene overexpression. Lin et al.[49] reported that over-expressed *ACS1* can significantly reduce acetate production as a byproduct while simultaneously reducing carbon consumption, redirecting carbon flux to the mevalonate pathway to synthesise terpenoids. Ni et al.[50] reported that *ADH2* overexpression reduced ethanol production and increased the yield of the terpenoid β-amyrin by 42.2%. Shi et al.[51] overexpressed *ALD6* and increased acetate levels, increasing the lycopene yield to 289 mg/L. It has also been found that mitochondrial acetyl-CoA and succinate can be converted into succinyl-CoA and acetate by overexpressing *ACH1*. The acetate is transported to the cytoplasm and then enters the PDH bypass pathway. (2) Branch pathway genes are knocked out, and reverse genes are over-expressed to inhibit acetyl-CoA loss. Ethanol and acetate are common acetyl-CoA products, and their production can be inhibited by gene knockout. Li et al.[37] reported that *ADH1* knockout directed metabolic flux to fatty acid synthesis, increasing fatty acid production by 1.9 times using the engineered bacteria DG005. Lian et al.[34] reduced ethanol production by inactivating one or more of the *ADH* genes (*ADH1–ADH5*), which increased acetyl-CoA levels and *n*-butanol yield by two- and fourfold, respectively. Alternatively, cells can save their metabolic flow by overexpressing reverse-synthesised genes. Chen et al.[4] changed the carbon flux from ethanol to acetate and acetate to acetyl-CoA by expressing *ADH2* and *ALD6*, thereby increasing the santalene yield by fourfold. (3) The cofactor NADPH concentration is regulated. For fatty acid synthesis, acetyl-CoA forms a primer that can be extended by adding a C2 unit derived from malonyl-CoA. Each additional C2 unit requires two reduction–oxidation (REDOX) cofactors, NADPH and NADPH, as byproducts, which increase acetyl-CoA production[52]. Cardenas et al.[53] combined two methods (the accumulation of NADPH combined with a reduction in the carbon flux into the mitochondria) and reported that the *S. cerevisiae* triacetate lactone titre was 6.4 times greater than that of nonengineered yeast strains. Overall, engineering strategies for the PDH bypass pathway mainly include increasing acetic acid levels, reducing ethanol generation, regulating ACS expression to promote acetyl-CoA synthesis from acetic acid, introducing other PDH bypass pathways, and improving cofactor supply. By combining these strategies, we can significantly increase acetyl-CoA levels and promote acetyl-CoA-derived compound production.

Finally, one of the key reasons for selecting mitochondrial function-deficient mutants is the integral role of mitochondria in cellular energy metabolism and their influence on lipid biosynthesis and degradation. Mitochondria are essential for ATP production through oxidative phosphorylation, and this energy production is intricately linked to the regulation of various metabolic pathways, including lipid metabolism[54]. Dysfunctional mitochondria can disrupt these processes, leading to alterations in lipid homoeostasis[55]. Therefore, by studying mutants with impaired mitochondrial function, we aimed to uncover both the direct and indirect effects of mitochondrial dysfunction on lipid metabolism pathways. Previous studies have demonstrated that mitochondrial dysfunction can significantly impact lipid metabolism[56,57]. For instance, mitochondrial defects have been associated with changes in fatty acid synthesis and the accumulation of lipid droplets[56]. In our study, we observed that mitochondrial function-deficient mutants exhibited distinct lipid profiles compared to wild-type strains. Specifically, we noted an increase in the accumulation of certain lipid species, suggesting a disruption in normal lipid metabolic processes. These findings provide further evidence supporting the critical role of mitochondria in regulating lipid metabolism, thereby validating our

choice of experimental model. *ALD4* is mainly derived from the analysis of MRDMs, but whether *ALD4* is also involved in the regulation of mitochondrial respiration is currently unclear. REDOX shuttles in the mitochondria, including ethanol–acetaldehyde shuttles, are important for respiratory growth[58]. Cha et al.[59] restored yeast respiratory defects by overexpressing *ALD4* using a heterologous promoter, thereby increasing ethanol utilisation and cell density. Although *ALD4* is only involved in ethanol degradation, glycerol utilisation was also restored, suggesting that *ALD4* overexpression alone can trigger cellular respiratory growth metabolism reprogramming. The mitochondrial fatty acid synthesis (mtFAS) pathway regulates mitochondrial respiratory chain function to meet the substrate availability (acetyl-CoA) requirements for the tricarboxylic acid cycle[60,61]. Neither functional cytoplasmic fatty acid synthesis nor exogenous fatty acid addition corrected the yeast respiratory-deficient phenotype[62], whereas only mitochondrial fatty acid-generated acyl-ACPs acted as signalling molecules in the metabolic state-sensing pathway within the mitochondria, coordinating mitochondrial acetyl-CoA levels with mitochondrial respiration[63]. Therefore, we suggest that *ALD4* may regulate acetyl-CoA metabolic pathways and mitochondrial respiration by participating in mtFAS synthesis.

In summary, understanding the mechanisms underlying the role of PDH bypass in metabolic flux is crucial for identifying metabolic engineering strategies to increase lipid biosynthesis. The advantages of this study are as follows: (1) a combined multi-omics analysis targeted key candidate genes that potentially regulate lipid metabolism at the population level; (2) regulation of *ALD4* to adjust the direction of PDH bypassing carbon flux, resulting in metabolic flux flowing to the synthesis of acetyl-CoA and ensuring sufficient precursor supply; (3) at the metabolic level, we demonstrate that *ALD4* is involved in lipid synthesis; and (4) based on the functional annotation of *ALD4*, regulatory strategies for different application scenarios are proposed. *ALD4* overexpression was used to produce oil, while *ALD4* knockout was used to produce alcohol. However, although *ALD4* overexpression can effectively promote the accumulation of the intermediate acetyl-CoA, the yield is not sufficient for subsequent synthesis of many high-value lipid metabolites by yeast. Therefore, future efforts should focus on simultaneously optimising various processes to increase the content of acetyl-CoA in the cytoplasm of *S. cerevisiae*. These processes include reducing the Crabtree effect, relieving the feedback inhibition of ACS, improving the enzyme activity of ACS, and introducing PDH pathways independent of ATP supply. The combination of the above strategies can obtain sufficient supply of acetyl-CoA in production practice, promote the synthesis of high-value lipid compounds, and lay a foundation for the further development of PDH.

Material and methods
Strains and plasmids
DNA integration was performed on the *S. cerevisiae* strain BY4741 (*MATaΔhis3Δleu2Δmet15Δura3*). The *S. cerevisiae* strain BY4741 was obtained from the American Type Culture Collection (Manassas, VA, USA; collection number: ATCC 4040002). Gene cloning was performed using *Escherichia coli* (*E. coli*) Trans1-T1 (purchased; Trans, CD501-02). The P416-GPD expression vector of *S. cerevisiae* used was purchased from the BioVector (Biovector Science Lab, Inc.) NTCC typical culture storage centre. Recombinant *E. coli* were cultured in Luria–Bertani (LB) broth media supplemented with antibiotics (100 μg mL^{-1} ampicillin). YPD medium (1% yeast extract, 2% peptone, and 2% glucose) was used for yeast culture. Ethanol fermentation medium (10 g/L yeast extract powder, 200 g/L glucose, 20 g/L peptone, 1 g/L KH$_2$PO$_4$, 1 g/L (NH$_4$)$_2$SO$_4$, and 1 g/L MgSO$_4$) was used to convert sugars. Synthetic complete drop-out medium supplemented with 2% D-glucose and without uracil (SD-URA) was used for the selection and cultivation of recombinant strains harbouring p416-GPD-URA-derived plasmids. All restriction enzymes were purchased from Thermo Scientific (Thermo Fisher Scientific, USA), and the Gibson Assembly® cloning kit and DNA polymerase were purchased from New England Biolabs (USA). The gel extraction kit D2000 was purchased from OMEGA (Madison, WI, USA). The primers used were purchased from Aoke Dingsheng Biotechnology (Beijing, China).

Plasmid construction and yeast transformation
The genomic DNA of *S. cerevisiae* was extracted using a Yeast Genomic DNA Extraction Kit (Solarbio, D1900, Beijing, China) according to the manufacturer's instructions. *ALD4* was amplified with the primers 416-*ALD4*F and 416-*ALD4*R. The p416-GPD vector backbone was digested with XhoI and XbaI before being reassembled with *ALD4* fragments to produce the recombinant plasmid p416-GPD-*ALD4* (Fig. S3A, B). The yeast plasmid p416-GPD indicates that the gene is under the control of the GPD1 promoter (GPD promoter). The GPD1 promoter, from the glyceraldehyde-3-phosphate dehydrogenase gene, is typically used for strong, constitutive gene expression. The recombinant product was transformed into Trans1-T1 receptor cells via thermal excitation and screened on ampicillin-containing plates. Clones from the transformed plates were subjected to colony polymerase chain reaction (PCR). Colonies containing the *ALD4* fragment were expanded and cultured, followed by extraction and sequencing of the plasmid using the primers 416-GAPF and 416-CYC1R (Table 2), confirming its orientation and sequence (Supplementary Files 1 and 2).

p416-GPD-*ALD4* was introduced into *S. cerevisiae* BY4741 using the lithium acetate method[64], the transformants were screened on SD-URA solid media (Fig. 3C), and several clones were selected for colony PCR. The recombinant expression strain was named *ald4-oe*. The SD-URA medium was purchased from Coolaber (Beijing, China).

Construction of yeast knockout strains
The upstream and downstream homologous arm primers of *ALD4* were designed for PCR amplification. Primers were designed using the pESC-LEU plasmid as a template, and homologous arms (~1000 bp) upstream and downstream of the *ALD4* gene ORF were added to both ends of the primers. *ALD4*F was the upstream primer, and *ALD4*R was the downstream primer (Table 2). The knockout component fragment containing the *ALD4* homologous arms was amplified by PCR (Fig. S3D) and purified using an OMEGA D2000-1 PCR product recovery kit. *S. cerevisiae* competent cells were prepared with a sorbitol solution (1 mol/L) by electroporation. The electroshock parameters were set to 1.5 kV/cm high-voltage pulses, 25 μF capacitance, 200 Ω resistance, and a duration of 5 min. The resuspended yeast was coated on the corresponding screening SD/Leu- plates (Fig. S3F), and a single colony after growth was extracted according to the Yeast Genomic DNA Extraction Kit for genomic DNA extraction and used for PCR validation. LEU YZF and LEU YZR primers (Table 2) were used to verify whether the knockout component had homologous recombined with the *S. cerevisiae* haploid genome. This set of primers was designed on an amplified fragment of the *ALD4*-knockout strain. If the ORF of *ALD4* in the transformants had been knocked out, the PCR product was hand banded, while the PCR using the genomic DNA of wild-type yeast BY4741 as the template did not have banding (Fig. S3E). The amplification results indicated that the BY4741 *ALD4* knockdown strain was successfully generated, which was named *Δald4*. The minimal SD base medium, DO supplement-Leu medium, and 1 M sorbitol solution were purchased from Coolaber (Beijing, China).

Determination of growth rate and fermentation parameters
Growth rate: the activated bacterial suspension was inoculated into 50-mL triangular bottles containing 25 mL of fresh YPD medium at 1% inoculum and incubated at 30 °C with 200 r/min oscillation. Samples were collected every 3 h to determine the absorbance value (OD$_{600}$ nm). The absorbance values were measured with an Epoch microplate spectrophotometer (Bio-Tek Gene5, USA).

Fermentation parameters: the bacteria were cultivated to the logarithmic stage before being transferred to 250-mL shake flasks containing 100 mL of fermentation medium. The initial OD$_{600}$ of the inoculum was 0.1 for the static culture. After 72 h of fermentation, CO$_2$ weight loss was

Table 2 | Primers used in the construction of yeast overexpression and knockout strains

Primers	Sequence (5′–3′)
416-*ALD4*F	CTTAGTTTCGACGGATTCTAGAATGTTCAGTAGATCTACGCTC
416-*ALD4*R	CATAACTAATTACATGACTCGAGTTACTCGTCCAATTTGGCAC
416-GAPF	GTATATAAAGACGGTAGGTATTG
416-CYC1R	GACTTCAGGTTGTCTAACTC
*ALD4*F	GAAGTATCTGGAAAACCAACCAAGAAAACTACAATAACAAAAATAAATAAAGCAACTGTGGGAATACTCAGGTATC
*ALD4*R	GTATGTAAGCATCGATTGGACACCAGGCTTATTGATGACCTTCACCATTATGGGAAATGGTTC
LEU YZF	GCCAGGTGACCACGTTGGTC
LEU YZR	GTGGTACTGTTGGAACCACCT

The italic format indicates the gene name.

Determination of protein levels and enzyme activity

After fermentation in an ethanol medium for 72 h, the yeast precipitation was collected and the enzyme activity and protein concentration were detected. The protein concentration was determined using Bradford's method[66], and the amount of protein in the solution was calculated from the absorbance value at 595 nm after staining with Coomassie brilliant blue dye (G-250).

Preparation of the cell extract: yeast fermentation broth (5 mL) was prepared and centrifuged at $8000 \times g$ for 5 min, and the cell precipitate was collected and dissolved in a phosphate-buffered solution. The acid-washed glass beads were added (the amount added was approximately the same as the volume of the yeast) using a vortex oscillator for the wall-breaking treatment; the mixture was oscillated for 30 s, placed in an ice bath for 1 min, subjected to 15 cycles, and centrifuged at $10,000 \times g$ for 20 min (at 4 °C). The supernatant (fixed to 1 mL) was collected as the crude extract of the enzyme solution, which was used for the subsequent determination of related indices with three replications. The enzyme activity was calculated per milligram of protein. All reagents were purchased from Solarbio® (Beijing, China), and all enzymes, coenzymes, and glass beads (425–600 μm) were purchased from Sigma-Aldrich (Merck, DEU).

For the mitochondrial K^+-ALDH enzyme activity assay, 1 mol L^{-1} Tris-HCl (pH 9.2), 20 mmol L^{-1} β-NAD, 100 mmol L^{-1} substrate acetaldehyde, 3 mol L^{-1} KCl, 1 mmol L^{-1} mercaptoethanol, and crude enzyme were allowed to react at 35 °C. The enzyme activity measured the conversion of NAD^+ to NADH by determining the change in absorbance at 340 nm over 5 min, as described by Modig et al.[67]. The enzyme activity was defined as a quantitative change of 0.001 in the OD_{340} nm/min at 35 °C.

Cytoplasmic Mg^{2+}-ALDH enzyme activity assay: 0.1 mol L^{-1} Tris-HCl (pH 7.5), 5×10^{-4} mol/L $NADP^+$, 0.1 mol L^{-1} $MgCl_2$, 2×10^{-3} mol L^{-1} acetaldehyde, and crude enzyme were allowed to react at 35 °C. The enzyme activity measured $NADP^+$ conversion to NADPH by determining the change in absorbance at 340 nm over 5 min, as described by Dickinson et al.[68]. The enzyme activity was defined as the amount of enzyme required to produce 1 μmol of NADPH/min at 35 °C and pH 7.5.

For the ADH enzyme activity assay, 0.1 mol L^{-1} glycine/NaOH (pH 10.0) buffer solution, 2.4 mmol L^{-1} NAD^+, 100 mmol L^{-1} ethanol, and crude enzyme were reacted at 25 °C. The enzyme activity measured the conversion of NAD^+ to NADH by determining the change in absorbance at 340 nm over 5 min, as described by Larroy et al.[69]. The enzyme activity was defined as the amount of enzyme needed to oxidise NAD^+ to produce 1 μmol of NADH at 25 °C for 1 min.

For the PDC enzyme activity assay, 200 mmol L^{-1} citrate buffer solution (pH 6.0), 1 mol L^{-1} sodium pyruvate, 6.4 mmol L^{-1} β-NADH, 200 U mL^{-1} ADH, and crude enzyme were reacted at 25 °C. The enzyme activity was measured as the change in absorbance at 340 nm over 5 min, as described by Wang et al.[70]. The enzyme activity was defined as the conversion of 1 μmol of pyruvate to acetaldehyde/min at 25 °C and pH 6.0.

Acetyl-CoA: an acetyl-CoA kit (ACA-2B-Y; Suzhou Comin Biotechnology Co., Ltd., China) was used to measure acetyl-CoA. We measured changes in the NAD(P)+/NAD(P)H ratios to determine their effects on the synthesis of acetyl-CoA. To measure acetyl-CoA content, we used a coupled-enzyme assay involving malate dehydrogenase and citrate synthase. The principle of the assay is as follows: malate dehydrogenase catalyses the conversion of malate and $NAD+$ to oxaloacetate and NADH. Subsequently, citrate synthase catalyses the reaction between acetyl-CoA and oxaloacetate to produce citrate and coenzyme A. By coupling these reactions, the acetyl-CoA content is proportional to the rate of NADH generation. The increase in absorbance at 340 nm, resulting from NADH production, reflects the acetyl-CoA content.

The kit contains the following reagents: malate dehydrogenase, malic acid, NAD^+, citrate synthase, and phosphate buffer. First, the yeast cells need to be ultrasonically disrupted in phosphate buffer (ice bath, 20% power or 200 W, sonication for 3 s, 10-s intervals, repeated 30 times). After disruption, centrifuge at $8000 \times g$, 4 °C for 10 min, and collect the supernatant. Next, prepare the working solution by mixing the four reagents used in the enzymatic reaction according to the specified ratio. Add the sample to be tested, mix thoroughly, and immediately record the absorbance at 340 nm at 20 s (A1) and 80 s (A2). Calculate ΔA = A2 − A1. Finally, use the formula for acetyl-CoA content recommended in the manual to determine the acetyl-CoA content of the sample.

Metabolite extraction, assay, and analysis

The *S. cerevisiae* BY4741, along with *ALD4* overexpression and knockout strains, were cultivated in an ethanol fermentation medium for 72 h. Approximately 10^7 bacteriophage bacterial cultures were quickly transferred to a quenching solution (glycerol salt solution, 3:2 [v/v] ratio) and centrifuged for 10 min at 4 °C to remove the supernatant. The samples were transferred into Eppendorf tubes with 1000 μL of extraction solution (methanol acetonitrile v/v = 1:1, internal standard concentration 20 mg/L) containing the internal standard in three batches (300, 300, 400 μL) and swirled for 30 s. Steel beads were added and processed for 10 min on a 45-Hz grinder, ultrasonicated for 10 min (in an ice-water bath), and allowed to stand for 1 h at −20 °C. The samples were then centrifuged at $12,000 \times g$ at 4 °C for 15 min. We carefully removed 500 μL of the supernatant from the electropolished tube, dried the extract in a vacuum concentrator, added 160 μL of the extract (acetonitrile–water v/v: 1:1) to redissolve the dried metabolite, vortexed for 30 s, ultrasonicated for 10 min in an ice-water bath, and then centrifuged the sample at 4 °C and $12,000 \times g$ for 15 min. We carefully removed 120 μL of the supernatant from a 2 mL injection vial and added 10 μL of each sample to mix into a quality control sample. Ten

microlitres of each sample were mixed into a quality control sample for testing.

The liquid-mass spectrometry system for metabolomics analysis consisted of a Waters Acquity UPLC I-Class PLUS system with a Waters Xevo G2-XS QTOF mass spectrometer and Acquity UPLC HSS T3 columns (1.8 μm 2.1*100 mm) purchased from Waters. The data collected using MassLynx V4.2 were used for metabolite characterisation and quantification, with data processing operations such as peak extraction and alignment performed using Progenesis QI software based on the Progenesis QI software online METLIN database and a public database for identification. Theoretical fragment identification was also performed within 100 and 50 ppm deviations in the parent and fragment ion mass numbers, respectively.

Gene expression analysis
To examine the effect of *ALD4* overexpression and knockout on PDH bypass, pathway-related genes were identified using quantitative reverse transcription PCR (RT-qPCR). A spin column yeast total RNA purification kit (Sangon Biotech, Shanghai, China) was used to extract total RNA according to the manufacturer's instructions. cDNA synthesis was performed using fastKing gDNA dispelling RT supermix (TIANGEN Biotech [Beijing] Co., Ltd., KR118-02). Quantification of the cDNA copy number was accomplished using a SYBR Green PCR Kit (TIANGEN Biotech [Beijing] Co., Ltd., FP205-02) with a QuantStudio design and analysis system (QuantStudio 5 real-time fluorescence qPCR instrument). Primer sequences were designed using Oligo ArchitectTM (http://www.oligoarchitect.com/Login.jsp) software. Three biological replicates were set up for each sample, and the relative gene transcript levels were determined using the $2^{-\Delta\Delta CT}$ method. *ACT1* was used as an internal reference to eliminate the effect of the cell number on the amount of RNA.

Statistical analyses
The data were analysed using Origin 2021 and GraphPad Prism 9 software, one-way analysis of variance, and the least significant difference method using SPSS 26.0 software. The statistical comparisons were performed using one-way ANOVA statistical significance was set at *$p < 0.05$, **$p < 0.01$, ***$p < 0.001$; ns, not significant. Biological replicates and numbers of independent experiments are provided in the legends. Each experiment was conducted independently at least three times.

Statistics and reproducibility
In Fig. 2, the experimental samples were divided into two groups. The first group was the population of MRDMs, which included three samples ResD-1, ResD-2, and ResD-4. The other group was the control group (the wild-type strain). Both sets of samples had three biological replicates to measure the transcriptome and six biological replicates to measure the lipidome. In Figs. 3–5, the experimental samples are divided into three groups. The first group was *ald4*-oe strain, the second group was Δ*ald4* strain, and the third group was control group (wild-type strain). Three biological replicates were set up in each group to measure phenotypic indexes. RT-qPCR was repeated independently three times. The metabolomic assay was performed using six independent replicates. For all the experimental results, no data were excluded from the analysis.

Reporting summary
Further information on research design is available in the Nature Portfolio Reporting Summary linked to this article.

Data availability
The original sequence data obtained through the transcriptome were deposited in the Beijing Big Data Centre Genome Sequence Archives, Institute of Genomics, Chinese Academy of Sciences, registered with number CRA001812 and can be accessed at https://ngdc.cncb.ac.cn/gsa/search?searchTerm=CRA001812. We have provided access to the numerical source data for all the figures in the manuscript, which will be stored in the Figshare repository https://doi.org/10.6084/m9.figshare.27201099.

References
1. Ko, Y. S. et al. Tools and strategies of systems metabolic engineering for the development of microbial cell factories for chemical production. *Chem. Soc. Rev.* **49**, 4615–4636 (2020).
2. Su, B. et al. Engineering a balanced acetyl coenzyme a metabolism in *Saccharomyces cerevisiae* for lycopene production through rational and evolutionary engineering. *J. Agric. Food Chem.* **70**, 4019–4029 (2022).
3. Yuan, J. F. & Ching, C. B. Mitochondrial acetyl-CoA utilization pathway for terpenoid productions. *Metab. Eng.* **38**, 303–309 (2016).
4. Chen, Y., Daviet, L., Schalk, M., Siewers, V. & Nielsen, J. Establishing a platform cell factory through engineering of yeast acetyl-CoA metabolism. *Metab. Eng.* **15**, 48–54 (2013).
5. Lin, P. et al. Direct utilization of peroxisomal acetyl-CoA for the synthesis of polyketide compounds in *Saccharomyces cerevisiae*. *ACS Synth. Biol.* **12**, 1599–1607 (2023).
6. Xu, Y. P. et al. De novo biosynthesis of salvianolic acid B in *Saccharomyces cerevisiae* engineered with the rosmarinic acid biosynthetic pathway. *J. Agric. Food Chem.* **70**, 2290–2302 (2022).
7. Pronk, J. T., Steensma, H. Y. & vanDijken, J. P. Pyruvate metabolism in *Saccharomyces cerevisiae*. *Yeast* **12**, 1607–1633 (1996).
8. Liu, W., Zhang, B. & Jiang, R. Improving acetyl-CoA biosynthesis in *Saccharomyces cerevisiae* via the overexpression of pantothenate kinase and PDH bypass. *Biotechnol. Biofuels* **10**, 41 (2017).
9. van Rossum, H. M., Kozak, B. U., Pronk, J. T. & van Maris, A. J. A. Engineering cytosolic acetyl-coenzyme A supply in *Saccharomyces cerevisiae*: pathway stoichiometry, free-energy conservation and redox-cofactor balancing. *Metab. Eng.* **36**, 99–115 (2016).
10. Koivuranta, K. et al. Enhanced triacylglycerol production with genetically modified *Trichosporon oleaginosus*. *Front. Microbiol.* **9**, 1337 (2018).
11. Boubekeur, S. et al. A mitochondrial pyruvate dehydrogenase bypass in the yeast *Saccharomyces cerevisiae*. *J. Biol. Chem.* **274**, 21044–21048 (1999).
12. Navarro-Avino, J. P., Prasad, R., Miralles, V. J., Benito, R. M. & Serrano, R. A proposal for nomenclature of aldehyde dehydrogenases in *Saccharomyces cerevisiae* and characterization of the stress-inducible *ALD2* and *ALD3* genes. *Yeast* **15**, 829–842 (1999).
13. Meaden, P. G. et al. The *ALD6* gene of *Saccharomyces cerevisiae* encodes a cytosolic, Mg^{2+}-activated acetaldehyde dehydrogenase. *Yeast* **13**, 1319–1327 (1997).
14. Tessier, W. D., Meaden, P. G., Dickinson, F. M. & Midgley, M. Identification and disruption of the gene encoding the K^+-activated acetaldehyde dehydrogenase of *Saccharomyces cerevisiae*. *FEMS Microbiol. Lett.* **164**, 29–34 (1998).
15. Wang, X. P., Mann, C. J., Bai, Y. L., Ni, L. & Weiner, H. Molecular cloning, characterization, and potential roles of cytosolic and mitochondrial aldehyde dehydrogenases in ethanol metabolism in *Saccharomyces cerevisiae*. *J. Bacteriol.* **180**, 822–830 (1998).
16. Wernig, F., Baumann, L., Boles, E. & Oreb, M. Production of octanoic acid in *Saccharomyces cerevisiae*: investigation of new precursor supply engineering strategies and intrinsic limitations. *Biotechnol. Bioeng.* **118**, 3046–3057 (2021).
17. Su, B., Song, D., Yang, F. & Zhu, H. Engineering a growth-phase-dependent biosynthetic pathway for carotenoid production in *Saccharomyces cerevisiae*. *J. Ind. Microbiol. Biotechnol.* **47**, 383–393 (2020).
18. Saint-Prix, F., Bonquist, L. & Dequin, S. Functional analysis of the *ALD* gene family of *Saccharomyces cerevisiae* during anaerobic growth on

glucose: the NADP$^+$-dependent Ald6p and Ald5p isoforms play a major role in acetate formation. *Microbiology* **150**, 2209–2220 (2004).

19. Remize, F., Andrieu, E. & Dequin, S. Engineering of the pyruvate dehydrogenase bypass in *Saccharomyces cerevisiae*: role of the cytosolic Mg^{2+} and mitochondrial K$^+$ acetaldehyde dehydrogenases Ald6p and Ald4p in acetate formation during alcoholic fermentation. *Appl. Environ. Microbiol.* **66**, 3151–3159 (2000).

20. Wang, X., Sa, N., Wang, F. H. & Tian, P. F. Engineered constitutive pathway in *Klebsiella pneumoniae* for 3-hydroxypropionic acid production and implications for decoupling glycerol dissimilation pathways. *Curr. Microbiol.* **66**, 293–299 (2013).

21. Chen, L. N., Li, Y. & Tian, P. F. Enhanced promoter activity by replenishment of sigma factor rpoE in *Klebsiella pneumoniae*. *Indian J. Microbiol.* **56**, 190–197 (2016).

22. Holyavkin, C. et al. Genomic, transcriptomic, and metabolic characterization of 2-phenylethanol-resistant *Saccharomyces cerevisiae* obtained by evolutionary engineering. *Front. Microbiol.* **14**, 1148065 (2023).

23. Aranda, A. & del Olmo, M. L. Response to acetaldehyde stress in the yeast *Saccharomyces cerevisiae* involves a strain-dependent regulation of several *ALD* genes and is mediated by the general stress response pathway. *Yeast* **20**, 747–759 (2003).

24. Parmar, J. H., Bhartiya, S. & Venkatesh, K. V. Characterization of the adaptive response and growth upon hyperosmotic shock in *Saccharomyces cerevisiae*. *Mol. Biosyst.* **7**, 1138–1148 (2011).

25. Singh, S. et al. Aldehyde dehydrogenases in cellular responses to oxidative/electrophilic stress. *Free Radic. Bio. Med.* **56**, 89–101 (2013).

26. Guo, X. P. et al. Quantitative multi-omics analysis of the effects of mitochondrial dysfunction on lipid metabolism in *Saccharomyces cerevisiae*. *Appl. Microbiol. Biotechnol.* **104**, 1211–1226 (2020).

27. Ganesan, S., Shabits, B. N. & Zaremberg, V. Tracking diacylglycerol and phosphatidic acid pools in budding yeast. *Lipid Insights* **8**, 75–85 (2015).

28. Boubekeur, S., Camougrand, N., Bunoust, O., Rigoulet, M. & Guerin, B. Participation of acetaldehyde dehydrogenases in ethanol and pyruvate metabolism of the yeast *Saccharomyces cerevisiae*. *Eur. J. Biochem.* **268**, 5057–5065 (2001).

29. Miyagi, H., Kawai, S. & Murata, K. Two sources of mitochondrial NADPH in the yeast *Saccharomyces cerevisiae*. *J. Biol. Chem.* **284**, 7553–7560 (2009).

30. Chen, Y., Zhang, Y., Siewers, V. & Nielsen, J. *Ach1* is involved in shuttling mitochondrial acetyl units for cytosolic C2 provision in *Saccharomyces cerevisiae* lacking pyruvate decarboxylase. *FEMS Yeast Res.* **15**, fov015 (2015).

31. Milke, L., Aschenbrenner, J., Marienhagen, J. & Kallscheuer, N. Production of plant-derived polyphenols in microorganisms: current state and perspectives. *Appl. Microbiol. Biotechnol.* **102**, 1575–1585 (2018).

32. Milke, L. & Marienhagen, J. Engineering intracellular malonyl-CoA availability in microbial hosts and its impact on polyketide and fatty acid synthesis. *Appl. Microbiol. Biotechnol.* **104**, 6057–6065 (2020).

33. Zhang, Q., Zeng, W. Z., Xu, S. & Zhou, J. W. Metabolism and strategies for enhanced supply of acetyl-CoA in *Saccharomyces cerevisiae*. *Bioresour. Technol.* **342**, 125978 (2021).

34. Lian, J. Z., Si, T., Nair, N. U. & Zhao, H. M. Design and construction of acetyl-CoA overproducing *Saccharomyces cerevisiae* strains. *Metab. Eng.* **24**, 139–149 (2014).

35. Xiao, T., Khan, A., Shen, Y., Chen, L. & Rabinowitz, J. D. Glucose feeds the tricarboxylic acid cycle via excreted ethanol in fermenting yeast. *Nat. Chem. Biol.* **18**, 1380–1387 (2022).

36. Shiba, Y., Paradise, E. M., Kirby, J., Ro, D. K. & Keasing, J. D. Engineering of the pyruvate dehydrogenase bypass in

37. Li, X. W. et al. Overproduction of fatty acids in engineered *Saccharomyces cerevisiae* for high-level production of isoprenoids. *Metab. Eng.* **9**, 160–168 (2007).

38. Li, X. W. et al. Overproduction of fatty acids in engineered *Saccharomyces cerevisiae*. *Biotechnol. Bioeng.* **111**, 1841–1852 (2014).

39. Qiu, J. et al. Boosting the cannabidiol production in engineered *Saccharomyces cerevisiae* by harnessing the vacuolar transporter BPT1. *J. Agric. Food Chem.* **70**, 12055–12064 (2022).

40. Shi, L. & Tu, B. P. Acetyl-CoA and the regulation of metabolism: mechanisms and consequences. *Curr. Opin. Cell Biol.* **33**, 125–131 (2015).

41. Liu, K., Zhang, X., Sumanasekera, C., Lester, R. L. & Dickson, R. C. Signalling functions for sphingolipid long-chain bases in *Saccharomyces cerevisiae*. *Biochem. Soc. Trans.* **33**, 1170–1173 (2005).

42. Mao, C. G., Xu, R. J., Bielawska, A. & Obeid, L. M. Cloning of an alkaline ceramidase from *Saccharomyces cerevisiae*: an enzyme with reverse (CoA-independent) ceramide synthase activity. *J. Biol. Chem.* **275**, 6876–6884 (2000).

43. Giudetti, A. M., Stanca, E., Siculella, L., Gnoni, G. V. & Damiano, F. Nutritional and hormonal regulation of citrate and carnitine/acylcarnitine transporters: two mitochondrial carriers involved in fatty acid metabolism. *Int. J. Mol. Sci.* **17**, 817–817 (2016).

44. Dong, Y., Hu, J., Fan, L. & Chen, Q. RNA-Seq-based transcriptomic and metabolomic analysis reveal stress responses and programmed cell death induced by acetic acid in *Saccharomyces cerevisiae*. *Sci. Rep.* **7**, 42659–42659 (2017).

45. Hiltunen, J. K., Chen, Z. J., Haapalainen, A. M., Wierenga, R. K. & Kastaniotis, A. J. Mitochondrial fatty acid synthesis - an adopted set of enzymes making a pathway of major importance for the cellular metabolism. *Prog. Lipid Res.* **49**, 27–45 (2010).

46. Henderson, C. M., Lozada-Contreras, M., Naravane, Y., Longo, M. L. & Block, D. E. Analysis of major phospholipid species and ergosterol in fermenting industrial yeast strains using atmospheric pressure ionization ion-trap mass spectrometry. *J. Agric. Food Chem.* **59**, 12761–12770 (2011).

47. Sitepu, I. R. et al. Manipulation of culture conditions alters lipid content and fatty acid profiles of a wide variety of known and new oleaginous yeast species. *Bioresour. Technol.* **144**, 360–369 (2013).

48. Klug, L. & Daum, G. Yeast lipid metabolism at a glance. *FEMS Yeast Res.* **14**, 369–388 (2014).

49. Tang, X. L., Feng, H. X. & Chen, W. N. Metabolic engineering for enhanced fatty acids synthesis in *Saccharomyces cerevisiae*. *Metab. Eng.* **16**, 95–102 (2013).

50. Lin, H., Castro, N. M., Bennett, G. N. & San, K. Y. Acetyl-CoA synthetase overexpression in *Escherichia coli* demonstrates more efficient acetate assimilation and lower acetate accumulation: a potential tool in metabolic engineering. *Appl. Microbiol. Biotechnol.* **71**, 870–874 (2006).

51. Ni, J., Zhang, G., Qin, L., Li, J. & Li, C. Simultaneously down-regulation of multiplex branch pathways using CRISPRi and fermentation optimization for enhancing β-amyrin production in *Saccharomyces cerevisiae*. *Synth. Syst. Biotechnol.* **4**, 79–85 (2019).

52. Shi, B. et al. Systematic metabolic engineering of *Saccharomyces cerevisiae* for lycopene overproduction. *J. Agric. Food Chem.* **67**, 11148–11157 (2019).

53. de Jong, B. W., Shi, S., Siewers, V. & Nielsen, J. Improved production of fatty acid ethyl esters in *Saccharomyces cerevisiae* through up-regulation of the ethanol degradation pathway and expression of the heterologous phosphoketolase pathway. *Microb. Cell Fact.* **13**, 39 (2014).

54. Cardenas, J. & Da Silva, N. A. Engineering cofactor and transport mechanisms in *Saccharomyces cerevisiae* for enhanced acetyl-CoA and polyketide biosynthesis. *Metab. Eng.* **36**, 80–89 (2016).

55. Hiltunen, J. K. et al. The biochemistry of peroxisomal β-oxidation in the yeast *Saccharomyces cerevisiae*. *FEMS Microbiol. Rev.* **27**, 35–64 (2003).

55. Dimmer, K. S. et al. Genetic basis of mitochondrial function and morphology in *Saccharomyces cerevisiae*. *Mol. Biol. Cell* **13**, 847–853 (2002).

56. Vamecq, J. et al. Mitochondrial dysfunction and lipid homeostasis. *Curr. Drug Metab.* **13**, 1388–1400 (2012).

57. Aon, M. A., Bhatt, N. & Cortassa, S. C. Mitochondrial and cellular mechanisms for managing lipid excess. *Front. Physiol.* **5**, 282 (2014).

58. Chen, X., Li, S. & Liu, L. Engineering redox balance through cofactor systems. *Trends Biotechnol.* **32**, 337–343 (2014).

59. Cha, S., Hong, C. P., Kang, H. A. & Hahn, J. S. Differential activation mechanisms of two isoforms of Gcr1 transcription factor generated from spliced and un-spliced transcripts in *Saccharomyces cerevisiae*. *Nucleic Acids Res.* **49**, 745–759 (2021).

60. Kursu, V. A. S. et al. Defects in mitochondrial fatty acid synthesis result in failure of multiple aspects of mitochondrial biogenesis in *Saccharomyces cerevisiae*. *Mol. Microbiol.* **90**, 824–840 (2013).

61. Van Vranken, J. G. et al. ACP acylation is an acetyl-CoA-dependent modification required for electron transport chain assembly. *Mol. Cell* **71**, 567–580 (2018).

62. Kastaniotis, A. J. et al. Mitochondrial fatty acid synthesis, fatty acids and mitochondrial physiology. *Biochim. Biophys. Acta Mol. Cell Biol. Lipids* **1862**, 39–48 (2017).

63. Masud, A. J., Kastaniotis, A. J., Rahman, M. T., Autio, K. J. & Hiltunen, J. K. Mitochondrial acyl carrier protein (ACP) at the interface of metabolic state sensing and mitochondrial function. *Biochim. Biophys. Acta Mol. Cell Res.* **1866**, 118540 (2019).

64. Gietz, D., Stjean, A., Woods, R. A. & Schiestl, R. H. Improved method for high-efficiency transformation of intact yeast-cells. *Nucleic Acids Res.* **20**, 1425–1425 (1992).

65. Varga, E., Klinke, H. B., Réczey, K. & Thomsen, A. B. High solid simultaneous saccharification and fermentation of wet oxidized corn stover to ethanol. *Biotechnol. Bioeng.* **88**, 567–574 (2004).

66. Bradford, M. M. Rapid and sensitive method for quantitation of microgram quantities of protein utilizing principle of protein-dye binding. *Anal. Biochem.* **72**, 248–254 (1976).

67. Modig, T., Lidén, G. & Taherzadeh, M. J. Inhibition effects of furfural on alcohol dehydrogenase, aldehyde dehydrogenase and pyruvate dehydrogenase. *Biochem. J.* **363**, 769–776 (2002).

68. Dickinson, F. M. The purification and some properties of the Mg^{2+}-activated cytosolic aldehyde dehydrogenase of *Saccharomyces cerevisiae*. *Biochem. J.* **315**, 393–399 (1996).

69. Larroy, C., Fernández, M. R., González, E., Parés, X. & Biosca, J. A. Characterization of the *Saccharomyces cerevisiae YMR318C (ADH6)* gene product as a broad specificity NADPH-dependent alcohol dehydrogenase: relevance in aldehyde reduction. *Biochem. J.* **361**, 163–172 (2002).

70. Wang, D. et al. Metabolic engineering of *Saccharomyces cerevisiae* for accumulating pyruvic acid. *Ann. Microbiol.* **65**, 2323–2331 (2015).

Acknowledgements

Author contributions

D.L., X.G., and C.L. conceived the project and designed the experiments. C.L., M.Z., J.R., and M.L. performed the research. C.L., X.G., M.Z., X.Z., N.D., J.R., C.J., Y.W., J.Z., Z.D., and D.L. analysed the data. C.L. and X.G. wrote the paper. D.L. and M.Z. acquired funding. All authors discussed the results and commented on the manuscript.

Competing interests

The authors declare no competing interests.

Additional information

Supplementary information The online version contains supplementary material available at https://doi.org/10.1038/s42003-024-07103-7.

Correspondence and requests for materials should be addressed to Xiaopeng Guo, Miaomiao Zhang or Dong Lu.

Peer review information *Communications Biology* thanks Shangtian Yang and the other, anonymous, reviewer(s) for their contribution to the peer review of this work. Primary handling editors: Cesar de la Fuente and Tobias Goris. A peer review file is available.

Reprints and permissions information is available at http://www.nature.com/reprints

Publisher's note Springer Nature remains neutral with regard to jurisdictional claims in published maps and institutional affiliations.